Buffer Layers for Superconducting Y-Ba-Cu-O Thin Films on Silicon and SiO_2

R. DE REUS* and F. W. SARIS
FOM-Institute for Atomic and Molecular Physics, Kruislaan 407, 1098 SJ Amsterdam (The Netherlands)
G. J. VAN DER KOLK, C. WITMER and B. DAM
Philips Research Laboratories, P.O. Box 80000, 5600 JA Eindhoven (The Netherlands)
D. H. A. BLANK, D. J. ADELERHOF and J. FLOKSTRA
University of Twente, P.O. Box 217, 7500 AE Enschede (The Netherlands)
(Received April 9, 1990)

Abstract

By direct deposition onto hot substrates, using laser ablation, crystalline $YBa_2Cu_3O_{7-\delta}$ (123) was obtained at 650 °C on SiO_2, but not on (100) Si substrates. The 123 film did not show a superconducting transition due to interfacial reactions. The failure temperature of insulating buffer layers, such as tantalum oxide and hafnium oxide, is around 500 °C. Although MgO and $BaZrO_3$ show a high stability in contact with 123 at 900 °C, they fail as a diffusion barrier at much lower temperatures. Below 400 °C barium diffuses through MgO, which itself remains unaffected. Using $BaZrO_3$ the same happens around 700 °C. BaF_2 fails as a diffusion barrier below 400 °C. Using laser ablation, high quality 123 films were grown on ZrO_2 buffer layers above 650 °C. For the first time we report superconducting transitions of 123 deposited at 650 °C onto an amorphous metal alloy, $Ir_{45}Ta_{55}$. The problems encountered using conducting buffer layers are either a low reaction temperature with 123 (HfB_2 and HfN) or oxidation of the metal alloy ($Ir_{45}Ta_{55}$) around 400 °C. Intermediate noble metal layers silver and Ag/Au/Ag could not prevent oxygen diffusion towards the underlying buffer layer.

1. Introduction

The use of high T_c superconductors in microelectronics, *e.g.* as passive interconnects or as superconductor/semiconductor devices, not only requires reliable and easy deposition processes on substrate materials as silicon and SiO_2, but also high stability of the superconductor against standard anneals in IC technology at 450-600 °C. The high reactivity of $YBa_2Cu_3O_{7-\delta}$ (henceforth abbreviated as 123) with various materials deteriorates the superconducting properties, especially when applied in thin film form.

Using laser ablation, sputtering, or electron gun evaporation, amorphous and insulating films are obtained at low deposition temperatures [1-3] and heat treatments in oxygen ambient at 850 °C are required to form the superconducting 123 phase. *In situ* preparation of superconducting 123 is possible by deposition in an oxygen background pressure at substrate temperatures of 650 °C and higher [4, 5]. By using oxygen plasmas even lower preparation temperatures can be achieved [6-8]. Although direct deposition of thin film 123 (less than 1 μm) onto silicon substrates has been reported by several authors [5, 6, 9, 10], the quality of the films is relatively poor. To obtain epitaxial films with high critical temperatures and currents, optimum deposition temperatures are found to be around 750 °C and (100) $SrTiO_3$ substrates should be used [11, 12]. To obtain high quality 123 films on silicon either a novel low temperature deposition technique or buffer layers which minimize interdiffusion between substrate and 123 are required.

To date, a great effort has been spent on the investigation of deposition techniques and the use of appropriate (mostly single-crystal) substrates, but not much is known about the applicability of thin film diffusion barriers. The most promising results are obtained with ZrO_2 buffer layers on silicon substrates [9], Al_2O_3 substrates [13], and oxidized silicon substrates (SiO_2) [14]. Supercon-

*Present address: Physics Department, Risø National Laboratory, DK-4000 Roskilde, Denmark.

0921-5107/90/$3.50 © Elsevier Sequoia/Printed in The Netherlands

ducting 123 thin films have also been prepared on MgO single crystals covered with Nb, Ag [15], or Au [16], and on SiO_2 covered with Ag [17]. Recently, epitaxial $MgAlO_2/SrTiO_3$ and $MgAlO_2/BaTiO_3$ buffer layer structures were successfully used to grow epitaxial 123 on (100) Si substrates [18, 19].

In this paper, we report on a variety of electrically conducting and insulating buffer layers and their stability against annealing in vacuum and oxygen flow. The films are in contact with thin film Y-Ba-Cu-O. Although this work is focused on reaction mechanisms and reaction temperatures, also a laser ablation technique was used in an effort to grow 123 on hot (100) Si and Si/SiO_2 substrates *in situ* with and without buffer layers. We report on the first observation of a superconducting transition of thin film 123 on an amorphous metal alloy, a-$Ir_{45}Ta_{55}$.

2. Experimental details

In this study, two types of experiments were performed. Firstly, reactions in sandwich structures with 123 on top of a buffer layer were investigated and secondly reactions in sample structures with overlayers on top of 123. Most buffer layers were deposited onto (100) Si and oxidized silicon substrates (SiO_2) using an r.f. diode sputtering apparatus. The typical thickness of the buffer layers was 0.2 μm. On top of the buffer layers 123 was deposited from a stoichiometric 123 bulk target ($T_c = 92$ K) with a triode sputtering apparatus described by Dam *et al.* [2]. Overlayers on top of a superconducting 123 phase were deposited in an electron gun evaporator. In this case the 123 was grown on (100) $SrTiO_3$ substrates by appropriate annealing of sputtered 123 films [2]. The thickness of the 123 films was usually 0.2 μm.

The following sample structures were prepared (see Table 1): Si/123, $Si/SiO_2/123$, Si/Ta-O/123, Si/Hf-O/123, $Si/SiO_2/MgO/123$, $Si/Si_3N_4/BaF_2/123$, $Si/SiO_2/BaZrO_3/123$, $SrTiO_3/123/a\text{-}Ir_{45}Ta_{55}$, $Si/a\text{-}Ir_{45}Ta_{55}/Ag/123$, $Si/a\text{-}Ir_{45}Ta_{55}/Ag/Au/Ag/123$, $Si/HfB_2/123$, $SrTiO_3/123/HfB_2$, and Si/HfN/123. Furthermore, $Si/SiO_2/BaZrO_3/123$ sample structures were prepared using electron gun deposition in which case the 123 film was codeposited using Y, Cu, and BaF_2 source materials. This method usually yields $T_c = 90$ K films after annealing in a

TABLE 1 Summary of the experiments presented in this paper. The thickness of the buffer layers as well as of the 123 films was usually 0.2 μm. When laser ablation was used, the failure temperature refers to the deposition temperature. Detailed information is given in the text

Sample	*Method*	*Failure*	*Remarks*
Si/123	Laser ablation	575 °C	Ba_2SiO_4 (?), no 123
	Post anneal	675 °C	Ba_2SiO_4 (?), no 123
$Si/SiO_2/123$	Laser ablation	650 °C	Ba_2SiO_4 (?), 123 formed
	Post anneal	675 °C	Ba_2SiO_4 (?), no 123
Si/a-TaO	Post anneal	> 800 °C	Crystalline Ta_2O_5 at 650 °C
Si/a-TaO/123	Post anneal	500-600 °C	$Ba_{0.5}TaO_3$ at 123 interface
$Si/Ta_2O_5/123$	Post anneal	500-600 °C	$Ba_{0.5}TaO_3$ at 123 interface
Si/a-HfO	Post anneal	> 800 °C	Crystalline HfO_2 at 500-600 °C
Si/a-HfO/123	Post anneal	< 500 °C	Both interfaces, $BaHfO_3$, Ba_2SiO_4 (?)
$Si/SiO_2/MgO/123$	Post anneal	< 400 °C	Barium pile up at SiO_2 interface
$Si/Si_3N_4/BaF_2/123$	Post anneal	< 400 °C	Intermixing at 123 interface, blistering
$Si/NiSi_2/ZrO_2/123$	Laser ablation	> 800 °C	Superconducting 123 above 650 °C
$Si/SiO_2/BaZrO_3/123$	Post anneal	700 °C	Ba_2SiO_4 at SiO_2 interface, $BaZrO_3$ stable, 123 degrades
$Si/SiO_2/BaZrO_3/123\text{-}F$	Wet post anneal	< 750 °C	Ba_2SiO_4 at SiO_2 interface, 123 formed
Si/a-IrTa/123	Laser ablation	675 °C	Cracks, superconducting 123
$SrTiO_3/123/a\text{-}IrTa$	Vacuum anneal	750 °C	Barium at surface
Si/a-IrTa/Ag/123	Post anneal	400 °C	Oxidation of Ir-Ta
		500 °C	Silver diffusion
		600-700 °C	Complete intermixing
Si/a-IrTa/Ag/Au/Ag/123	Post anneal	< 400 °C	Gold and silver intermix, Ir-Ta oxidizes
		600-700 °C	Complete intermixing
$SrTi_3/123/HfB_2$	Vacuum anneal	< 700 °C	Oxygen at surface
$Si/HfB_2/123$	Post anneal	< 650 °C	Complete intermixing
Si/HfN	Post anneal	700 °C	HfON formation
Si/HfN/123	Post anneal	< 500 °C	Complete intermixing

wet oxygen flow at 850 °C [3]. To minimize interfacial reactions, we reduced the annealing temperature to 750 °C, which usually yields superconducting 123 films with critical temperatures of at least 76 K. The choice of the buffer layers will be discussed later.

Direct deposition of 123 onto (100)Si, Si/SiO_2, $Si/a\text{-}Ir_{45}Ta_{55}$, and $Si/NiSi_2/ZrO_2$ substrates at elevated temperatures was done using a laser ablation technique as described in refs. 1, 4, 12 and 20. The amorphous Ir–Ta was deposited in an electron gun evaporator and the $Si/NiSi_2/ZrO_2$ substrates were obtained by annealing electron-gun-deposited amorphous Ni–Zr in an oxygen ambient. The $NiSi_2$ is epitaxial with the (111)Si substrate and the ZrO_2 is polycrystalline, see ref. 21.

For the laser ablation process a XeCl excimer laser was used, which was operated at a repetition rate of 1 Hz. The laser beam entered the deposition chamber through a quartz window incident near 45° to the target surface normal and was focused on the target resulting in a laser power fluence of approximately 2 J cm^{-2}. The sample was positioned in front of the target at a distance of 3 cm. The background pressure of the laser deposition system was less than 1×10^{-4} Pa. During deposition, oxygen was introduced to the system close to and directed towards the sample surface to a pressure of 10 Pa, as measured 30 cm away from the oxygen inlet. Typical deposition times were between 30 min and 1 h, resulting in 123 layers with thicknesses ranging from 0.5 to 1 μm. The substrate temperature was measured

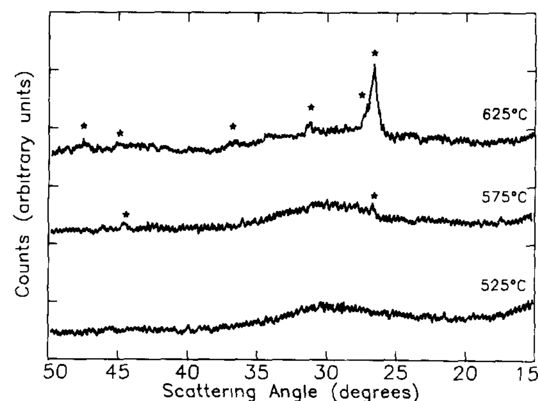

Fig 1. XRD spectra of 123 directly deposited onto (100) Si at elevated temperatures by laser ablation. At low temperatures amorphous 123 was formed. At 575 °C and higher temperatures a crystalline compound (indicated by symbols) was formed because of reaction. No 123 was detected.

using a pyrometer. Immediately after deposition, oxygen was let into the system at atmospheric pressure and the sample was cooled down slowly to 450 °C. At this temperature it was kept for 1 h before cooling to room temperature.

Post annealing of the samples was carried out in an oxygen flow or *in situ* in vacuum directly after deposition. Analysis was done using: 2 MeV $^4He^+$ Rutherford backscattering spectrometry (RBS) with the aid of the RUMP computer code [22], X-ray diffraction (XRD) with Cu Kα radiation in a conventional $\theta - 2\theta$ diffractometer, and Auger electron spectroscopy (AES).

After deposition of gold contacts, electrical resistivities were measured as a function of temperature. A four-point probe method was applied using a d.c. current between 1 and 500 μA.

3. Results and discussion

3.1. Direct deposition of 123 on Si and SiO_2

Laser ablation was used to deposit 123 directly onto (100) Si at elevated temperatures. All films deposited had a black and shiny appearance. In Fig. 1 XRD spectra are shown of 123 films deposited at various temperatures. After deposition at 525 °C the films appear to be amorphous as can be concluded from the broad feature around the 30° scattering angle. At a substrate temperature of 575 °C not only the amorphous phase, but also some crystalline material is observed. The peaks arising from the crystalline phase, indicated in Fig. 1 by symbols, increase in intensity at higher deposition temperatures. The phase could not be identified but is probably a barium silicate. There was no evidence for the formation of crystalline 123. The results were reproducible and do not change if the oxygen pressure is varied between 0.05 and 1.0 mbar during deposition.

RBS measurements (not shown) indicate that the composition of the deposited films is stoichiometric 123 within the error bars of the measurement (3%). At 575 °C and higher temperatures an interfacial reaction was observed, resulting in barium depletion of the 123 film.

Annealing amorphous 123, deposited by laser ablation onto (100)Si at 400 °C, for 1 h in an oxygen flow results in formation of Ba_2SiO_4 at temperatures higher than 675 °C, according to XRD; no crystalline 123 was obtained.

On the Si/SiO_2 substrates it was possible to grow crystalline 123. This is shown in the XRD spectra of Fig. 2. Deposition at 600 °C yielded an

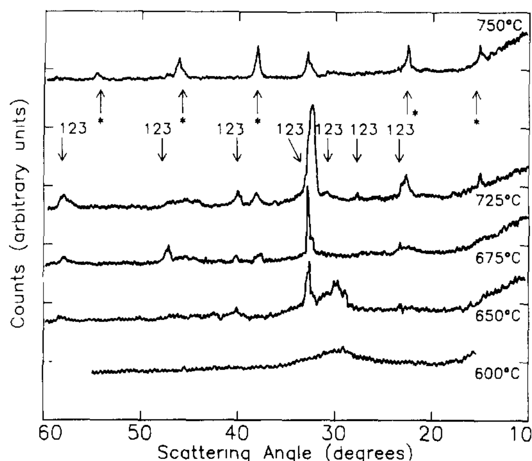

Fig 2. XRD spectra of 123 directly deposited onto SiO_2 at elevated temperatures by laser ablation At 650 °C a mixture of amorphous and crystalline 123 was deposited. At higher temperatures crystalline 123 and an unidentified reaction product (indicated by asterisks) are observed. The reaction product dominates after deposition at 750 °C

amorphous phase, but at 650 °C part of the as-deposited film contained crystalline 123. The peak positions of the strongest reflections of polycrystalline 123 are indicated in the figure. During deposition of 675 °C no amorphous phase, but crystalline 123 formed. Also an unidentified phase started to form, different from the one observed when silicon substrates were used. The peak positions of this phase are indicated by asterisks. After deposition at 725 °C strong reflections of both 123 and the unidentified phase were observed. After deposition at 750 °C the latter phase is dominant.

In agreement with our XRD results, interfacial reactions were observed with RBS (not shown) in samples deposited at temperatures of 675 °C and higher.

Post annealing in an oxygen flow of amorphous 123 films, prepared by laser ablation, on Si/SiO_2 substrates lead to Ba_2SiO_4 formation at temperatures of 675 °C and higher, as observed by XRD and RBS.

A summary of the results described above is given in Table 1. In contrast with reports in the literature [5, 6, 9, 10] we were not able to deposit crystalline 123 films with a thickness less than 1 μm onto (100) Si. Although Venkatesan *et al.* [9] reported only a slight intermixing of silicon and barium at the Si/123 interface, we have observed interfacial reactions at temperatures lower than those required to deposit crystalline 123.

Post annealing at 800 °C of amorphous and insulating 123 films on silicon yields heavily reacted samples, as reported in the literature [23, 24]. Nakajima *et al.* [24] reported the formation of copper silicide. In a powder mixture of silicon and the superconducting 123 phase, the 211 Y-Ba-Cu-O phase was observed primarily after annealing between 600 and 800 °C in an oxygen flow by Cheung and Ruckenstein [25]. In our case neither of these phases were observed. This was also the case for post annealing of the Si/a-123 samples.

Our data on deposition of 123 onto SiO_2 are consistent with observations by Venkatesan *et al.* [9]. Although interdiffusion of silicon and barium during deposition of 700 °C strongly affected the stoichiometry, crystalline 123 was formed.

The inconsistency of the various results on direct deposition of 123 on silicon and SiO_2 probably indicates that the processing parameters to form the superconducting 123 phase are very critical. A small misorientation of the silicon substrate might have dramatic consequences for the reactivity with 123. Also the oxygen content, which is near stoichiometry in our samples, might play a role in the reactivity of the 123. Our results on SiO_2 show that in a very narrow temperature range between 650 and 675 °C crystalline 123 is deposited without the formation of any other phases. There is no chance of growing 123 on silicon or SiO_2 by post annealing at 850 °C. Appropriate buffer layers are needed to overcome these problems. In the following sections we will discuss a number of buffer layers.

3.2. *Insulating buffer layers*

The electrically insulating buffer layers we have tested were as follows: Ta-O, Hf-O, MgO, BaF_2, ZrO_2 and $BaZrO_3$. Tantalum oxide was studied rather extensively. Its large heat of formation suggests a high chemical stability. Because the same results were obtained for tantalum deposited in an electron gun evaporator, as well as for Ta-O deposited by reactive sputtering, we only report the results of the electron-gun-deposited samples. In Fig. 3(a) RBS measurements are shown which were obtained after annealing Si/Ta samples in an oxygen flow. Surface peak positions for various elements are indicated by arrows. In the spectrum of an as-deposited sample (solid line) a well defined tantalum peak is observed at the surface peak position, whereas the silicon substrate signal is found at energies lower than the corresponding surface peak position. Tantalum oxidation started during

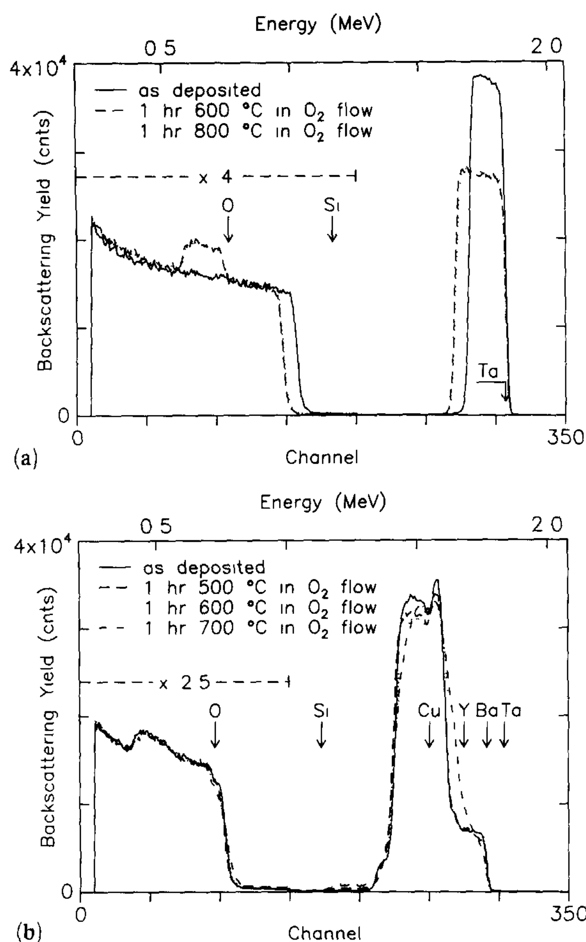

Fig. 3. (a) RBS spectra of Si/Ta samples obtained with 2 MeV He^+ backscattering. Scattering angle is 170°, sample tilt 7°. Oxidation of tantalum is observed without intermixing at the interface. (b) as (a) for Si/Ta–O/123 samples. In the temperature range from 500 to 600 °C 123 and the Ta–O buffer layer intermix.

annealing for 1 h at 400 °C. After annealing for 1 h at 500 °C, the tantalum top layer was fully oxidized as can be seen by the decrease in yield and the broadening of the tantalum peak caused by oxygen which is observed at the surface peak position. Only slight changes were observed at higher annealing temperatures. After annealing at 600 and 800 °C, the RBS spectra appear to be identical. The composition of the Ta–O formed is close to that of stoichiometric Ta_2O_5. Because of the extra stopping introduced by the oxygen, the silicon signal has shifted to lower energies with respect to the silicon signal in the spectrum of the as-deposited sample. The silicon interface remained unaffected as can be inferred from the slopes of the silicon signal and tantalum trailing edge.

From XRD (not shown) we have learned that below 650 °C an amorphous Ta–O is formed. At higher temperatures the only phase observed was randomly oriented Ta_2O_5.

Both amorphous Ta–O and Ta_2O_5, prepared at 500 and 700 °C as described above, were tested as a buffer layer between (100)Si and sputtered amorphous 123. RBS spectra obtained after annealing Si/Ta–O/123 sample structures in an oxygen flow are shown in Fig. 3(b). In the spectrum of an as-deposited sample (solid line) Y, Ba, Cu, and O signals from the 123 top layer are observed at their surface peak positions; they partially overlap with the tantalum signal of the Ta–O buffer layer, which is shifted to lower energies with respect to the surface backscattering energy. The spectrum obtained after annealing at 500 °C (broken line) is almost identical with the spectrum of the as-deposited sample. This indicates that no interdiffusion has occurred. During annealing at 600 °C (dotted line) intermixing of Ta–O and 123 has taken place as can be concluded by the changes in the tantalum leading edge (close to the Y surface peak position). No changes are observed at the silicon interface. After annealing at 700 °C, more reaction is observed. A little foot in the silicon signal indicates that reaction at the silicon interface has also occurred.

In XRD spectra from Si/Ta–O/123 samples annealed at 700 °C $Ba_{0.5}TaO_3$ could be identified.

Using Ta_2O_5 instead of amorphous Ta–O as a buffer layer yielded very similar results with comparable reaction temperatures and reaction products.

Also the results (not shown) obtained from experiments with sputtered Hf–O buffer layers were similar to those with Ta–O. RBS measurements showed that Hf–O is inert in contact with silicon upon annealing in oxygen flow up to at least 800 °C. XRD showed that at low temperatures an amorphous Hf–O is formed which crystallized into HfO_2 between 500 and 600 °C. As a buffer layer between silicon and amorphous 123, the Hf–O film already failed at the lowest annealing temperature of 500 °C. At this temperature interdiffusion was observed at both the silicon and 123 interface by RBS. One of the reaction products identified with XRD was $BaHfO_3$.

We have also performed experiments with sputtered polycrystalline MgO buffer layers, because single crystalline MgO has been proven

to be a suitable substrate. In Fig. 4 RBS spectra are shown for $Si/SiO_2/MgO/123$ sample structures annealed in an oxygen flow. The thickness of the sputtered 123 film in this case was 0.1 μm. Yttrium, barium, copper and oxygen signals are observed at the surface peak positions. Already after annealing at 400 °C (broken line) it can be seen, by the decrease in the barium surface peak, that the concentration of barium in the 123 layer has decreased by a large amount. This barium is found at the SiO_2/MgO interface (indicated in Fig. 4), whereas the MgO appears to be unaffected. The same process is observed after annealing at 500 and 600 °C. After annealing at 700 °C (dotted line), copper has also diffused into the underlying substrate and both the SiO_2/MgO and MgO/123 interfaces have degraded.

From XRD measurements (not shown) it could be seen that crystalline MgO was present in all samples as deposited and annealed. Although reaction was observed at temperatures as low as 400 °C, only above 600 °C a crystalline phase, most likely Ba_2SiO_4, was formed.

RBS measurements on $Si/Si_3N_4/BaF_2/123$ sample structures (not shown) revealed that BaF_2 and 123 readily intermixed during annealing at 400 °C in oxygen flow. In addition, blistering of the films was observed (even with the naked eye). During annealing at 500 °C the $BaF_2/123$ film peeled off from the Si_3N_4 substrate.

Deposition of 123 onto $Si/NiSi_2/ZrO_2$ substrates (see ref. 21), using laser ablation, yielded crystalline 123 at substrate temperatures higher than 650 °C. Figure 5 shows an RBS spectrum obtained from a sample deposited at 780 °C. Yttrium, barium, copper and oxygen are observed at the sample surface in the right stoichiometry. The sharp peak just below the copper signal arises from backscattering from zirconium in the ZrO_2 buffer layer. The smaller peak at slightly higher energies than the silicon surface backscatter energy is due to nickel from the epitaxial $NiSi_2$. The silicon signal can be found at lower energies. From the RBS spectrum it can be inferred that all interfaces are sharp and that hardly any interdiffusion has occurred.

XRD on the $Si/NiSi_2/ZrO_2/123$ samples showed that although the ZrO_2 is polycrystalline a highly oriented 123 layer was grown with the *c* axis normal to the surface. A detailed study on the characterization of the 123 film and interfacial reactions in these sample structures will be published elsewhere [26]. The reader is also referred to section 3.4.

In Fig. 6 RBS spectra of vacuum annealed $SiO_2/BaZrO_3/123$ samples are shown. Prior to sputter deposition of the 123 film the 0.4 μm thick $BaZrO_3$ buffer layer was annealed at 800 °C in oxygen ambient to ensure the right stoichiometry. After annealing $SiO_2/BaZrO_3/123$ at 650 °C in vacuum (solid line), the sample structure was very well preserved. Steps in the spectrum at the yttrium, barium and copper surface peak positions and the separate appearance of a zirconium peak from the buffer layer (visible in the trailing edge of the metal peak) indicate that hardly any interdiffusion has occurred. The surface of the 123 film seems to be slightly deficient in barium

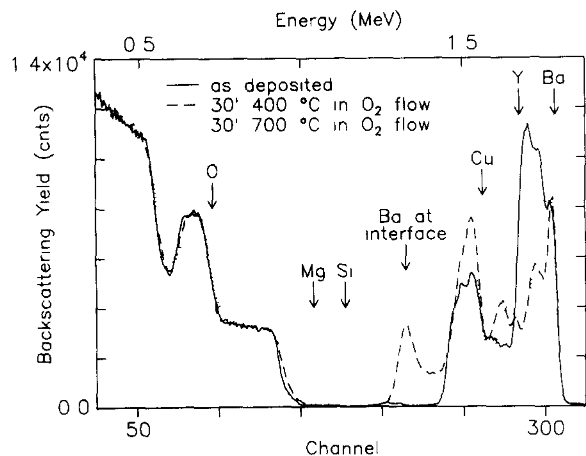

Fig. 4. RBS spectra for $SiO_2/MgO/123$ sample structures. At 400 °C barium piled up at the SiO_2 interface whereas the MgO remained unaffected. Copper interdiffusion occurred at 700 °C.

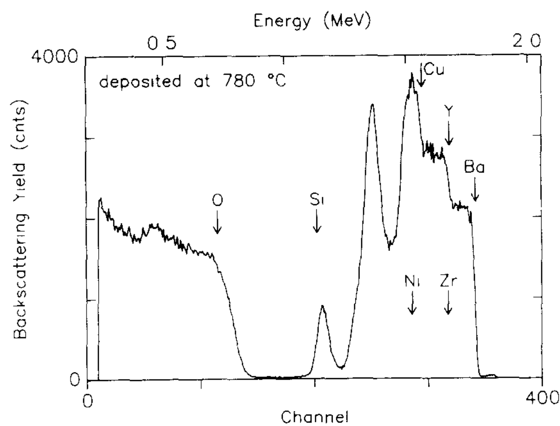

Fig. 5. RBS spectra for a laser-ablated 123 film deposited at 780 °C onto $Si/NiSi_2/ZrO_2$ samples. The 123 film is stoichiometric and no interfacial reactions are observed

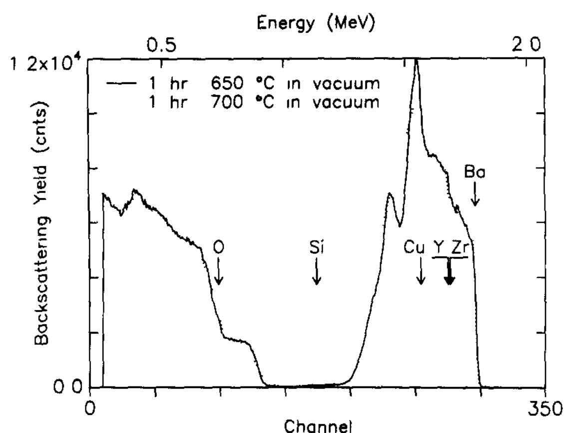

Fig. 6. RBS spectra for $SiO_2/BaZrO_3/123$ samples annealed in vacuum. Failure of the buffer layer occurred between temperatures of 650 and 700 °C.

as can be deduced from the increasing yield of the barium signal from the surface peak position towards lower energies, *i.e.* deeper into the sample. After annealing at 700 °C (dotted line), the steps in the spectrum at the yttrium, barium and copper surface peak positions are still visible; the backscattering signal from zirconium cannot be distinguished anymore. Also, some silicon interdiffusion is observed as can be seen by the decrease in slope of the silicon signal, which is found at lower energies. XRD showed that in the sample annealed at 700 °C a small amount of crystalline 123 was present.

Similar samples were prepared using BaF_2, copper and yttrium sources in an electron gun evaporator to deposit the 123 film. XRD on this type of samples, annealed in a wet oxygen flow at the reduced temperature of 750 °C to substitute the fluorine in the 123 film by oxygen, demonstrated the presence of polycrystalline 123. Using RBS, however, a considerable amount of interdiffusion between silicon and barium was observed as well.

In Table 1 the results on insulating buffer layers are summarized. BaF_2 appears to be unsuccessful as a buffer layer for forming crystalline 123. Severe interdiffusion was observed at low annealing temperatures and the adhesion to Si_3N_4 is bad.

Also, Ta–O and Hf–O seem to be unsuitable because of their relatively low reaction temperatures with 123. The formation of barium-tantalate and barium-hafnate is not unexpected since these reactions are exothermic. The large negative heats of formation of Ta_2O_5 and HfO_2 (-299 kJ mol^{-1} and -374 kJ mol^{-1} respectively, see ref. 27) suggest a high chemical stability of the oxides. However, a lower reaction temperature for Hf–O as compared with Ta–O has been experimentally observed. This shows that one cannot predict reaction temperatures using the criterion of a high formation enthalpy of the buffer layer alone. The mobility of the reactant, in this case barium, is dominant.

Although single-crystal MgO and ZrO_2 are both successful substrates and have been proven to be very inert in contact with 123 [24, 25], it was possible to grow crystalline 123 on thin film ZrO_2, whereas a thin layer of polycrystalline MgO was not able to prevent diffusion of barium into the underlying SiO_2. The $NiSi_2$ in the $Si/NiSi_2/ZrO_2/123$ samples did not participate in any reaction. Probably the different preparation techniques for the ZrO_2 (thermal oxidation) and the MgO (sputtering) influence the density of the buffer layer which will facilitate grain boundary diffusion. The use of thicker MgO buffer layers might be a solution to this problem.

$BaZrO_3$ has been found to be less stable than ZrO_2 as a buffer layer. This can be explained as follows. $BaZrO_3$ is the reaction product of ZrO_2 and 123 at temperatures higher than 800 °C [25, 28]. Therefore no reactions are to be expected between $BaZrO_3$ and 123, in agreement with observations by Cima *et al.* [28]. $SiO_2/BaZrO_3$ sample structures are likewise very stable against annealing up to at least 800 °C, as was observed after preparing the buffer layer. Because both $SiO_2/BaZrO_3$ and $BaZrO_3/123$ do not show any reaction, $BaZrO_3$ seems to be an ideal buffer layer in $SiO_2/BaZrO_3/123$ sample structures. Unfortunately, at 700 °C Ba_2SiO_4 formed in $SiO_2/BaZrO_3/123$ samples at the SiO_2 interface. The barium involved in the reaction was supplied from the 123 top layer, which showed barium depletion. Because $BaZrO_3$ is the most stable phase in the sample structure, the only way for the system to lower its free energy is to form Ba_2SiO_4 by reacting SiO_2 and 123. Barium is highly mobile (see, for example, the experiments with the MgO buffer layer), so it can pass easily through the $BaZrO_3$ buffer layer. Because barium is already present at the SiO_2 interface in the $SiO_2/BaZrO_3/123$ samples a reaction is to be expected at the temperature at which SiO_2 and 123 react, which is around 675 °C. This is indeed the failure temperature observed for the $SiO_2/BaZrO_3/123$ sample structures. However, if the

buffer layer consists of ZrO_2, the SiO_2 substrate and barium (in 123) are separated. Before SiO_2 and barium can react, first the complete ZrO_2 buffer layer has to be consumed to form $BaZrO_3$ in a reaction with the 123 top layer. This reaction occurs at temperatures higher than 800 °C [25, 28], which makes ZrO_2 a better buffer layer than $BaZrO_3$.

Assuming the same reaction mechanism, also $Ba_{0.5}TaO_3$ and $BaHfO_3$ are expected to fail as a diffusion barrier in contact with silicon or SiO_2 at the reaction temperatures of Si/123 and SiO_2/123 respectively. In conclusion, oxides which do not contain barium, such as ZrO_2 or $SrTiO_3$, are most stable for use as an insulating buffer layer.

3.3. Conducting buffer layers

123 was deposited directly on electron-gun-deposited a-$Ir_{45}Ta_{55}$ at elevated temperatures using laser ablation. At a deposition temperature of 650 °C, crystalline 123 layers with a thickness of 0.5 μm were obtained which had a black and smooth appearance. The peaks of this polycrystalline 123 film are indicated in the XRD spectrum of Fig. 7. Apart from the 123 phase, only peaks from the silicon substrate and gold contacts are detected. Also, amorphous Ir–Ta–O is observed which appears as a broad feature with low intensity between scattering angles of 20° and 30°. In samples obtained at deposition temperatures between 675 and 750 °C 123 and the crystalline oxides Ta_2O_5 and IrO_2 are observed. In addition, the film showed cracks. The oxidation of the buffer layer and crack formation above 700 °C have also been observed in a previous study on post annealing of Si/a-$Ir_{45}Ta_{55}$/123 sample structures. In that case a mixture of the 123 and 211 phases was obtained at 850 °C [29].

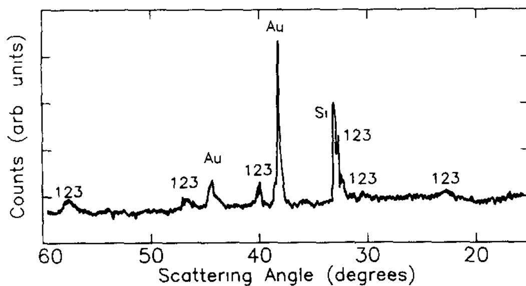

Fig 7. XRD spectrum of a 123 film deposited onto Si/a-$Ir_{45}Ta_{55}$ samples at 650 °C using laser ablation. The a-$Ir_{45}Ta_{55}$ oxidized during deposition. The gold peaks are from contacts deposited after deposition.

We have studied the annealing behaviour of Ir–Ta layers on top of the crystalline superconducting 123 phase. Prior to electron gun deposition of the 0.1 μm thick amorphous Ir–Ta, the samples were annealed in oxygen to obtain the superconducting 123 compound. RBS as well as AES showed that barium appeared at the surface of the $SrTiO_3$/123/a-$Ir_{45}Ta_{55}$ samples after annealing for 15 min at temperatures greater than 750 °C in a vacuum of 1×10^{-7} Pa.

Because the severe oxidation of the Ir–Ta buffer layer will destroy its conductive properties we have tried to minimize the oxygen indiffusion by adding a silver buffer layer between the Ir–Ta and 123. Figure 8(a) shows RBS measurements on annealed Si/a-$Ir_{45}Ta_{55}$/Ag samples without a

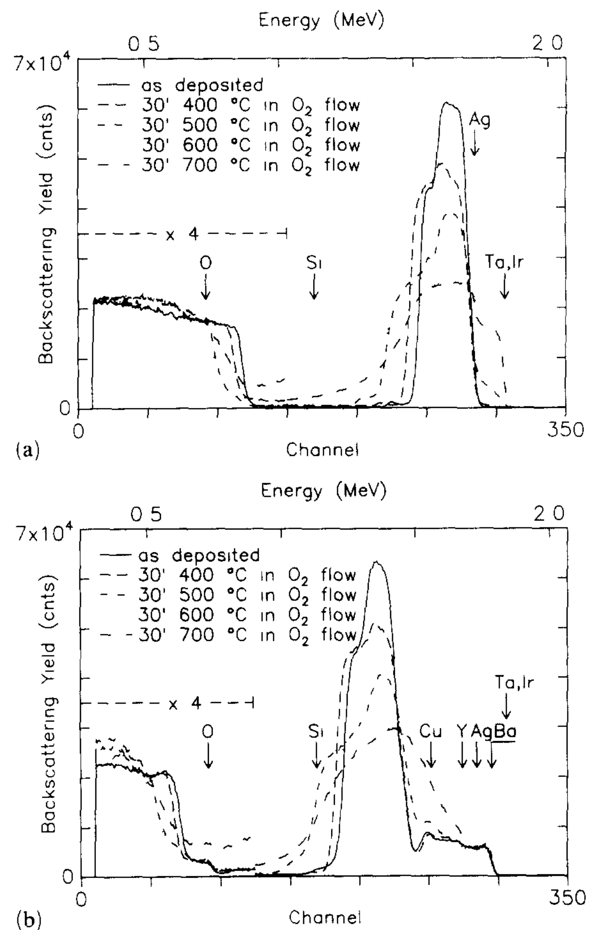

Fig. 8. (a) RBS spectra for Si/a-$Ir_{45}Ta_{55}$/Ag samples Oxidation of the a-$Ir_{45}Ta_{55}$ is observed at all annealing temperatures. Intermixing of silicon and Ag with the buffer layer occurred at 500 °C and higher temperatures. Complete failure is observed at 700 °C. (b) As (a) but now with 123 top layer. Oxidation of the a-$Ir_{45}Ta_{55}$ occurred already at 400 °C At 500 °C mainly silver has intermixed with the neighbouring Ir–Ta–O and 123 Complete failure occurred at 700 °C

123 top layer. In the spectrum of the as-deposited sample (solid line) a silver signal is found at the surface peak position. This signal overlaps with the Ir–Ta signal which can be recognized as a step in the trailing edge of the peak. Backscattering signals from indium and tantalum cannot be distinguished with 2 MeV He^+ RBS since both elements have almost the same mass. At lower energies the signal due to silicon is observed. No oxygen is observed in the as-deposited samples. After annealing for 30 min at 400 °C (broken line), oxygen is observed in part of the Ir–Ta layer. The silicon signal is shifted to lower energies because of the oxygen incorporated in the surface layer. At this temperature the silicon and silver interfaces were stable. During annealing at 500 °C more oxidation was observed; Ir–Ta appeared at the sample surface and the silicon interface started to degrade. These effects became more pronounced at higher annealing temperatures, as can be observed in the spectrum obtained after annealing at 600 °C. At 700 °C, the sample structure has intermixed almost completely.

Results for the same samples covered with 123 are shown in Fig. 8(b). In the spectrum of the as-deposited Si/a-$Ir_{45}Ta_{55}$/Ag/123 sample (solid line) yttrium, barium and copper signals are found at the corresponding surface peak positions. The part of the spectrum at lower energies is essentially the same as described above for the samples without 123. At 400 °C, the Ir–Ta oxidized; the interface between Ag and 123 is still sharp. After annealing at 500 °C, not only oxidation of the Ir–Ta is observed, but interdiffusion of silver with the 123 top layer and Ir–Ta bottom layer as well. Again, during annealing at 700 °C severe intermixing with the silicon substrate occurred.

We have tried to retard the oxidation of the Ir–Ta, replacing the single silver layer by a Ag/Au/Ag sandwich structure on top of the Ir–Ta. The RBS spectra of these Si/Ir–Ta/Ag/Au/Ag sample structures (Fig. 9(a)) are rather complicated. In the spectrum of an as-deposited sample (solid line) a silver peak is observed at the surface peak position. The silver top layer shifts the gold signal to lower energies. The gold signal causes a step in the silver trailing edge. The second peak, at lower energies, is due to backscattering from silver from the bottom silver layer and Ir–Ta, which causes the step in the trailing edge of this second peak. The silicon substrate signal is found

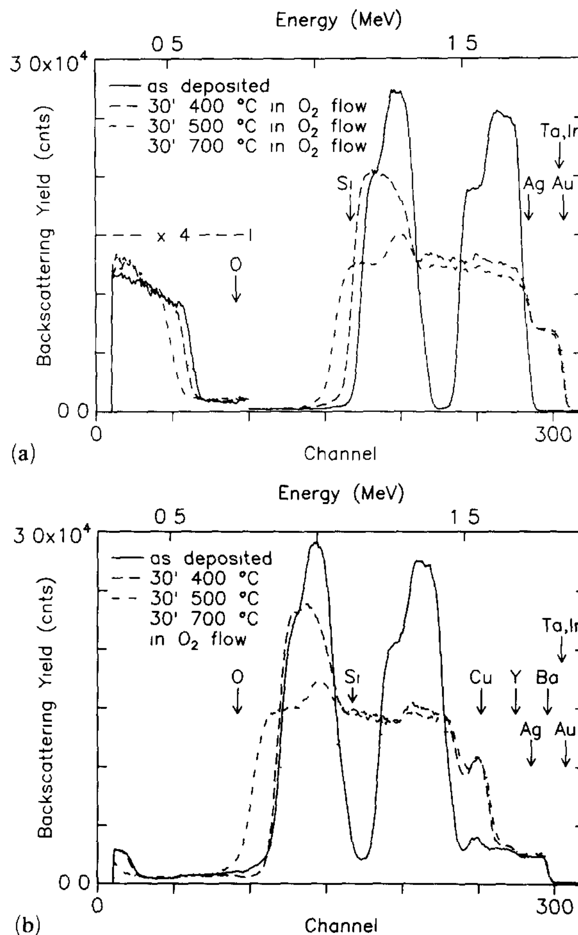

Fig. 9. (a) RBS spectra as in Fig. 8, but the silver layer is replaced by an Ag/Au/Ag sandwich structure. Gold and silver have intermixed completely at 400 °C and oxidation of the a-$Ir_{45}Ta_{55}$ started. Only during annealing at 700 °C was the silicon interface affected. (b) The same samples as in Fig. 9(a) covered with a 123 top layer. Although again the a-$Ir_{45}Ta_{55}$ was oxidized and the Ag/Au/Ag structure completely intermixed, the interfaces with the 123 top layer and silicon substrate remained sharp below 700 °C.

at lower energies. After annealing for 30 min at 400 °C in an oxygen flow (broken line), it is found that the Ag/Au/Ag structure has completely intermixed. The Ir–Ta signal is now visible as a peak at energies slightly higher than the silicon surface peak position. Oxidation of the Ir–Ta has set in and the oxygen can just be seen at the lowest energies in the spectrum on top of the silicon substrate signal. The interfaces between the Ir–Ta and the silicon substrate and the Ag–Au mixture on top remained sharp. After annealing at 500 °C, the interfaces were still sharp but the Ir–Ta oxidized. The same behaviour was found after annealing at 600 °C; complete intermixing occurred at 700 °C.

In Fig. 9(b) RBS spectra are shown which were measured after annealing Si/Ir–Ta/Ag/Au/Ag/123 sandwich structures. The results are very similar to those obtained without 123. During annealing at 400 °C the silver and gold intermixed and part of the Ir–Ta layer oxidized. In contrast to the experiment with the single silver layer no interdiffusion of silver and 123 was observed. The spectrum after annealing at 400 °C (broken line) is a similar spectrum as obtained without the 123 layer (see Fig. 9(a), broken line), but it is shifted backwards in energy from the gold down to the copper surface peak positions and superimposed on the signal from the Y–Ba–Cu. After annealing at 500 and 600 °C, the Ir–Ta was fully oxidized, whereas at the silicon and 123 interface slight intermixing with the buffer layer had occurred. At 700 °C, the complete sandwich structure had intermixed.

A few measurements (not shown) were performed on another conducting buffer layer, HfB_2, because its high heat of formation might be a sufficiently high barrier against reaction with 123. AES on a $SrTiO_3$/123/HfB_2 sample annealed for 15 min at 700 °C in a vacuum of 1×10^{-7} Pa revealed the presence of oxygen at the sample surface. This oxygen was supplied from the 123 layer and reached the surface after diffusing through the 0.2 μm thick HfB_2 top layer. Annealing at 650 °C in an oxygen ambient of Si/HfB_2/123 samples resulted in severe intermixing as observed with RBS.

Furthermore, HfN exhibits a high heat of formation and might perform well as a diffusion barrier. Therefore, Si/HfN and Si/HfN/123 samples were annealed in an oxygen flow and examined with RBS and XRD (not shown). It appeared that the as-deposited HfN was crystalline and epitaxial with the (100)Si substrate. The samples were stable against annealing for 1 h at temperatures up to 600 °C. At 700 °C, the HfN oxidized and an epitaxial and stoichiometric hafnium-oxynitride (HfON) formed. To our knowledge this compound has not been reported in the literature. The conducting HfN layer between silicon and 123 behaved very similar to the HfO_2 buffer layer upon annealing in an oxygen flow. Already at the lowest annealing temperature of 500 °C failure of the diffusion barrier at both the silicon and 123 interfaces was observed and the amount of intermixing increased with increasing annealing temperature.

A summary of the results on conducting buffer layers and their failure temperatures is given in Table 1. Thin films of amorphous $Ir_{45}Ta_{55}$ exhibit crystallization temperatures as high as 900 °C in vacuum [30, 31]. Their stability against annealing in contact with silicon is very good. In vacuum no reactions between silicon and a-$Ir_{45}Ta_{55}$ occur below 875 °C [32] and Si/a-$Ir_{45}Ta_{55}$/Au sample structures survive annealing procedures at 600 °C for 24 h in atmospheric ambient [33]. It has been reported earlier that a-$Ir_{45}Ta_{55}$ as a diffusion barrier between silicon and 123 avoids interfacial reactions up to at least 650 °C [29]. However, a strong oxidation was observed similar to the experiments performed in this work. Upon crystallization of the amorphous Ir–Ta–O complex above 650 °C cracks were observed. The absence of extended defects in the amorphous phases strongly retards the diffusion of various elements along fast diffusion paths such as grain boundaries and dislocations at moderate temperatures. This offers the possibility to grow crystalline 123 on amorphous Ir–Ta at deposition temperatures as high as 650 °C, as shown in our laser ablation experiments. However, the oxidation of the buffer layer might seriously affect the conducting properties, which makes the layer unsuitable as contacting material.

Silver was chosen in an attempt to avoid oxidation of the buffer layer for several reasons. It has been reported that oxygen diffusion in silver only becomes significant around 600 °C [34]. Also, incorporation of silver in 123 does not degrade the critical temperature [35] and no compound formation has been observed at temperatures as high as 945 °C [25]. Superconducting thin film 123 was successfully prepared on MgO single crystals covered with silver [15]. Furthermore, the adhesion of silicon to 123 is good and a silver contacting layer between the buffer layer and 123 is expected to be metallic. Although annealing in an oxygen ambient to 400 °C does not seem to affect the silver film, oxygen diffused through the silver layer and reacted with Ir–Ta. Apparently, silver is inert to oxygen but is not able to avoid diffusion of oxygen towards reactive material such as Ir–Ta. Above 500 °C, considerable amounts of silver diffuse into both the Ir–Ta buffer layer and the 123 top layer.

Gold is highly inert and expected to be a better barrier against oxygen than silver. Superconducting 123 films have been grown on gold-covered MgO substrates [16]. Because the adhesion of gold is rather poor we have sandwiched the gold

film between silver. The phase diagram of the Au–Ag system [36] shows that gold and silver form solid solutions over the full composition range. In our experiments this already happens at temperatures of 400 °C or lower. Like silver, also the Au–Ag layer did not prohibit oxygen diffusion into the Ir–Ta buffer layer, whereas the Au–Ag mixture itself remained unaffected. The interfaces of the Au–Ag mixture were found to be more stable than in the case of pure silver. During annealing at 600 °C, neither interdiffusion of Au–Ag with Ir–Ta–O nor with 123 occurred. Therefore, the Au–Ag solid solution can be used as a stable contacting material with good adhesive properties.

HfB_2 and HfN, which should be representative for refractory metal borides and nitrides, show rather similar behaviour as HfO_2. Unfortunately, the reaction temperature with 123 is too low for possible application as a buffer layer. Similarly, as in the case of Ir–Ta, oxidation of the buffer layer is a serious problem. At 700 °C HfON formed, a compound which has not been reported before to our knowledge.

It seems that depositing contact layers onto superconducting 123 films is not a problem as far as interfacial reactions are concerned. Major problems arise when formation of superconducting 123 on conducting buffer layers is desired because severe oxidation will destroy the conducting properties of the buffer layer in most cases. The amorphous refractory metal alloy Ir–Ta is a good example for showing this behaviour: it is possible to grow crystalline 123 but the buffer layer oxidized. We were not able to avoid oxygen diffusion into the samples by inserting noble metal diffusion barriers between 123 and the buffer layer. A solution to this problem may be the use of conducting oxides, like RuO_2 or Mo–O, as a buffer layer, but strong interfacial reactions might be expected as well, as was shown for Ta_2O_5 and HfO_2. Another suggestion is the use of amorphous refractory metal alloys containing one or more constituents which will yield conductive oxides during processing of the 123 top layer. This may be realized using amorphous Co–Mo or W–Ru, for which crystallization temperatures of respectively, 900 °C (ref. 37) and 800 °C (ref. 30) have been reported.

3.4. Electrical properties

After depositing gold films as contacts, resistivities were measured as a function of temperature using a four-point probe. The 123 films deposited directly onto SiO_2 substrates were all semiconducting. Neither transitions in the resistivity *vs.* temperature (R–T) curves nor in the a.c. susceptibility were observed above 5 K. Apparently, the interdiffusion between substrate and 123, which resulted in the formation of barium silicate, prohibits superconductivity.

The 123 films obtained on the insulating $BaZrO_3$ buffer layers at least partially reacted with the substrate and no superconducting transitions were measured in this case either. However, on ZrO_2 the 123 layers were rather easily grown and showed sharp transitions in the R–T curves. In Fig. 10 an example is given for a sample which was prepared with laser ablation at a deposition temperature of 725 °C. The 123 film shows a metallic behaviour at temperatures higher than 91 K, which is the onset temperature for superconductivity. Below this temperature a sharp decrease in the resistivity is observed and zero resistivity is obtained below 84 K. These results compare favourably with results given in the literature concerning ZrO_2 buffer layers [9, 14]. In a forthcoming publication [26] the influence of the processing parameters on the quality of the 123 film and the interfacial reactions occurring in the $Si/NiSi_2/ZrO_2/123$ samples will be reported.

Amorphous Ir–Ta is a candidate for use as a conducting buffer layer. The reaction temperature with 123 is rather high (approximately 700 °C) and we were able to form crystalline 123 films. However, the contact of the Ir–Ta deposited onto the superconducting 123 phase appeared to be semiconducting. This is probably

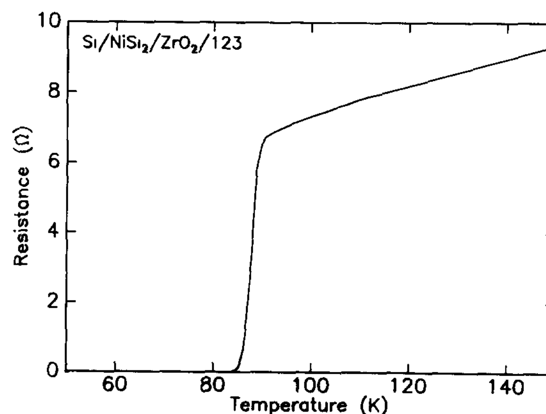

Fig. 10. R–T curve for a 123 film deposited onto $Si/NiSi_2/ZrO_2$ at 725 °C with laser ablation. Metallic behaviour is found at high temperatures. A resistivity drop set in at 91 K. Zero resistivity is obtained below 84 K.

caused by local oxidation of the buffer layer at the interface with the 123 film. Insertion of a thin silver layer might be a solution to this problem at low temperatures, for oxygen penetrates silver at 400 °C, as was shown above. The R–T curve for a laser-ablated 123 film onto amorphous Ir–Ta at a deposition temperature of 650 °C is shown in Fig. 11. During cooling of the sample a slight increase in the resistivity is observed. At an onset temperature of 90 K the resistivity drops and a rather broad transition is observed. At 25 K the resistivity reaches a minimum value of 1×10^{-3} Ω and remains constant upon cooling to liquid helium temperatures. The resistivity drops by four orders of magnitude upon cooling down from room temperature to 25 K. Clearly, the superconducting 123 phase is present, which is the first time that thin film superconducting 123 (0.5–1.0 μm) on amorphous metal alloys has been reported.

4. Conclusions

A number of conducting and insulating buffer layers for deposition of 123 on silicon and SiO_2 have been investigated. Direct deposition of 123 onto (100)Si and Si/SiO_2 substrates yielded crystalline 123 on the Si/SiO_2 substrates but no superconductivity was measured, whereas under identical circumstances high quality 123 films are obtained on ZrO_2 buffer layers. We attribute this difference in quality of the 123 layer to interfacial reactions between 123 and silicon or SiO_2. For reliable deposition of high quality 123 films on

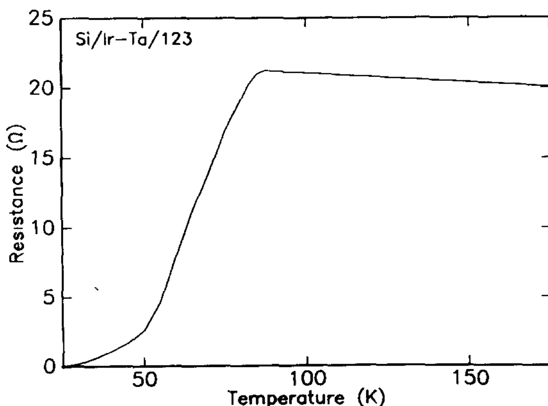

Fig. 11 R–T curve for a 123 film deposited onto Si/a-$Ir_{45}Ta_{55}$ at 650 °C with laser ablation. Weak semiconducting behaviour is observed at high temperatures. At 90 K the resistivity drops to reach a minimum (non-zero) value which remains constant below 25 K.

these types of substrates buffer layers are necessary.

The insulating buffer layers Ta–O and Hf–O failed at relatively low temperatures, which makes them unsuitable as buffer layers. Thin-film-sputtered MgO was inert to amorphous 123, however, diffusion of barium towards the underlying SiO_2 substrate could not be avoided. BaF_2 reacted with 123 at temperatures of 400 °C or lower. The performance of ZrO_2 as a buffer layer was very good and high quality 123 was formed. The barium-containing $BaZrO_3$ is highly stable against annealing when in contact with 123 only, but loses its properties as a buffer layer when in contact with SiO_2 because barium is passed from the 123 through the buffer layer and reacts with the substrate. For this reason buffer layers should not contain barium.

HfB_2 and HfN failed as conducting buffer layers for 123. At 700 °C HfN oxidizes and the compound HfON is formed, which has not been reported in the literature before. Both HfN and HfON are epitaxial with the (100)Si substrate. For the first time superconducting 123 has been grown on an amorphous metal alloy, $Ir_{45}Ta_{55}$. Although a clear transition in the R–T curve was observed at 90 K, no complete zero resistivity was obtained. In general, a major problem for the use of conducting buffer layers is the oxidation of most buffer layers containing transition metals. This will destroy the electrical properties of the buffer layer and its contact to the 123 films. This has been clearly demonstrated for Ir–Ta. Intermediate silver and Ag/Au/Ag layers could not prevent the Ir–Ta layer from oxidizing. Although silver readily diffuses into 123 and Ir–Ta–O at 500 °C, no interdiffusion is observed for a Au–Ag mixture below 700 °C. So, this Au–Ag mixture forms a stable contacting material with good adhesive properties.

The use of thin film amorphous metal alloys containing elements which will form conducting oxides may be a solution to the oxidation problems of the buffer layer. Because of the absence of grain boundaries, fast diffusion paths are not present and it may be possible to avoid interdiffusion and grow thin film crystalline 123 onto the amorphous buffer layer, as shown here for Ir–Ta.

Acknowledgments

We would like to thank A. C. Moleman, W. Moolhuyzen (University of Amsterdam), and

C. Langereis (Philips, Eindhoven) for their assistance with the XRD measurements. We acknowledge W. A. M. Aarnink and G. Gerritsma (University of Twente) for their valuable suggestions and analysis of the $Si/NiSi_2/ZrO_2/123$ sample structures. Also, we gratefully acknowledge T. S. Baller (Philips, Eindhoven), who participated in the experiments with the Ir–Ta buffer layer. This work is part of the research program of the Stichting voor Fundamenteel Onderzoek der Materie (Foundation for Fundamental Research on Matter) and was financially supported by the Nederlandse Organisatie voor Wetenschappelijk Onderzoek (Netherlands Organization for Scientific Research) and the Stichting Technische Wetenschappen (Netherlands Technology Foundation).

References

1 D. Dijkkamp, T. Venkatesan, X. D. Wu, S. A. Shaheen, N. Jisrawi, Y. H. Min-Lee, W. L. McLean and M. Croft, *Appl. Phys. Lett., 51* (1987) 619.
2 B. Dam, H. A. M. van Hal and C. Langereis, *Europhys. Lett., 5* (1988) 455.
3 B. Dam, G. M. Stollman, P. Berghuis, S. Q. Guo, C. F. J Flipse, J. G. Lensink and R. P. Griessen, *AIP Conf. Proc., 182* (1989) 172.
4 X. D. Wu, A. Inam, T. Venkatesan, C. C. Chang, E. W. Chase, P. Barboux, J. M. Tarascon and B. Wilkins, *Appl. Phys Lett, 52* (1988) 754.
5 P. Berberich, J. Tate, W. Dietsche and H. Kinder, *Appl. Phys. Lett., 53* (1988) 925.
6 R. M. Silver, A. B. Berezin, M. Wendman and A. L de Lozanne, *Appl. Phys. Lett., 52* (1988) 2174.
7 R. K. Singh, J. Narayan, A. K. Singh and J. Krisnaswamy, *Appl. Phys. Lett., 54* (1988) 2271.
8 S. Witanachchi, H. S. Kwok, X. W. Wang and D. T. Shaw, *Appl. Phys. Lett., 53* (1988) 234.
9 T. Venkatesan, E. W. Chase, X. D. Wu, A. Inam, C. C. Chang and F. K. Shokoohi, *Appl. Phys. Lett., 53* (1988) 243.
10 G. Koren, E. Polturak, B. Fischer, D. Cohen and G. Kimel, *Appl. Phys. Lett., 53* (1988) 2330.
11 H. C. Li, G. Linker, F. Ratzel, R. Smithey and J. Geerk, *Appl Phys. Lett., 52* (1988) 1098.
12 B. Roas, L. Schultz and G. Endres, *Appl. Phys. Lett., 53* (1988) 1557.
13 A. Stamper, D. W. Greve, D. Wong and T. E. Schlesinger, *Appl. Phys. Lett., 52* (1988) 1746.
14 A. Mogro-Campero, L. G. Turner, E. L. Hall and M. C. Burrell, *Appl. Phys. Lett., 52* (1988) 2068; A. Mogro-Campero, L. G. Turner and G. Kendall, *Appl. Phys. Lett., 53* (1988) 2566.
15 M. Gurvitch and A. T. Fiory, *Appl. Phys. Lett., 51* (1987) 1027.
16 C. L. Chien, G. Xiao, F. H. Streitz, A. Gavrin and M. Z. Cieplak, *Appl. Phys Lett., 51* (1987) 2155.
17 C.-A. Chang, C. C. Tsuei, T. R. McGuire, D. S. Yee, J. P. Boresh, H. R. Lilienthal and C. E. Farrell, *Appl. Phys. Lett., 53* (1988) 916
18 S. Miura, T. Yoshitake, S. Matsubara, Y. Miyasaka, N. Shohata and T. Satoh, *Appl. Phys. Lett., 53* (1988) 1967
19 X. D. Wu, A. Inam, M. S. Hegde, B. Wilkens, C. C. Chang, D. M. Hwang, L. Nazar, T. Venkatesan, S. Miura, S. Matsubara, Y. Miyasaka and N. Shohata, *Appl. Phys. Lett, 54* (1989) 754
20 T. S. Baller, G. N. A. van Veen and H. A. M. van Hal, *Appl. Phys, A46* (1988) 215.
21 R. de Reus, H. C. Tissink and F. W Saris, *J. Mater. Res., 5* (1990) 341.
22 L. R. Doolittle, *Nucl. Instrum. Meth., B9* (1985) 344.
23 B. Dam, T. S. Baller, G. N. A. van Veen, H. A M. van Hal, J. W. C. de Vries and G. M. Stollman, *MRS Symp. Proc., 99* (1988) 303.
24 H. Nakajima, S. Yamaguchi, K. Iwasaki, H. Morita and H. Fujimori, *Appl. Phys. Lett., 53* (1988) 1437.
25 C. T Cheung and E. Ruckenstein, *Mater. Lett., 7* (1988) 172.
26 W. A. M. Aarnink, D. H. A. Blank, D. J. Adelerhof, J. Flokstra, H. Rogalla, A. van Silfhout, R. de Reus and F. W. Saris, to be published.
27 M.-A. Nicolet and S. S. Lau, in N. G. Einspruch and G. B. Larrabee (eds.), *VSLI Electronics: Microstructure Science*, Academic, New York, 1983, p. 329.
28 M. J. Cima, J. S. Schneider, S. Peterson and W. Coblenz, *Appl. Phys. Lett., 53* (1988) 710.
29 R. de Reus, F. W. Saris and T. S. Baller, *J. Less-Common Met., 145* (1988) 217.
30 A. W. Denier van der Gon, J. C. Barbour, R. de Reus and F. W. Saris, *J Appl. Phys., 61* (1987) 1212.
31 G. J. van der Kolk, *J. Mater. Res., 3* (1988) 209.
32 R. de Reus, J. C. Barbour and F. W. Saris, *Mater Sci. Eng., B7* (1990) in the press.
33 A. G. Todd, P. G. Harris, I. H. Scobey and M. J. Kelly, *Solid State Electron, 27* (1984) 507.
34 W. Eichenauer and G. Müller, *Z. Metallkde., 53* (1962) 321.
35 R. Prasad, N. C. Soni, A. Mohan, S. K. Khera, K. U. Nair, C. K. Gupta, C V. Tomy and S. K. Malik, *Mater. Lett., 7* (1988) 9.
36 T. B. Massalski (ed.), *Binary Alloy Phase Diagrams*, American Society for Metals, Metals Park, OH, 1986.
37 L. S. Hung, F. W. Saris, S. Q. Wang and J. W. Mayer, *J. Appl. Phys., 59* (1986) 2416; S. Q. Wang, L. S. Hung and J. W. Mayer, *Thin Solid Films, 162* (1988) 199.